ADAM, An Aeroservoelastic Analysis Method for Analog or Digital Systems

Thomas Noll,* Maxwell Blair,† and John Cerra‡
Air Force Wright Aeronautical Laboratories, Wright-Patterson Air Force Base, Ohio

Coupling of the elastic modes and the high-gain automatic flight control systems of aircraft can result in unstable interactions within the flight envelope. These instabilities are any undamped structural oscillations sensed by the flight controller and driven by the control surface motions. This paper highlights the activities pursued by the Flight Dynamics Laboratory (FDL) in developing analysis tools for performing independent audits of proposed flight systems and for conducting research in the area of aeroservoelasticity (ASE). ADAM (Analog and Digital Aeroservoelasticity Method) combines the technologies of unsteady aerodynamics, multi-input/multi-output (MIMO) controls and structural dynamics into an interactive analysis package. The governing equations and the results of several examples that were used to verify the credibility of ADAM are discussed.

Nomenclature

$[a_i]$ = coefficient of aeroelastic equations of motion in the s-domain
$\ddot{a}_1, \ddot{a}_2, \ddot{a}_3$ = vertical accelerations
A = reference area
$[A]$ = state-space matrix
b = reference semichord
$[b_i]$ = coefficient of forced aeroelastic equations of motion in the s-domain
$[B]$ = state-space input matrix
$[C]$ = state-space output matrix
$[\bar{C}]$ = modal participation coefficient matrix
$[C_{sc}]$ = generalized damping matrix for control surface degrees of freedom (DOF)
$[C_{ss}]$ = generalized damping matrix for rigid body and elastic mode DOF
$[D]$ = state-space feed forward matrix
D_i = denominator coefficients of Pade polynomial
$F(\omega)$ = frequency response
h = displacement
i = imaginary, $\sqrt{-1}$
$[I]$ = identity matrix
k = reduced frequency, $b\omega/V$
$[K_{sc}]$ = generalized stiffness matrix for control surface DOF
$[K_{ss}]$ = generalized stiffness matrix for rigid body and elastic mode DOF
ℓ_{12}, ℓ_{13} = distance between sensors $\ddot{a}_1$ and $\ddot{a}_2$, and $\ddot{a}_3$ and $\ddot{a}_1$
$[M_{sc}]$ = generalized mass matrix for control surface DOF
$[M_{ss}]$ = generalized mass matrix for rigid body and elastic mode DOF
N_i = numerator coefficients of Pade polynomial
n = nth time step
q_c = generalized coordinate for control surface DOF
q_s = generalized coordinate for rigid body and elastic mode DOF
$[Q_{sc}]$ = generalized aerodynamic force matrix for control surface DOF
$[Q_{ss}]$ = generalized aerodynamic force matrix for rigid body and elastic mode DOF
Q_{ij} = element of the generalized aerodynamic force matrix
s = Laplace variable
t = time
t_0 = initial time
T = sampling time of digital system
u = state-space input
V = velocity
x = state-space variable
y = state-space output
z = z-domain variable
α = angular acceleration
ρ = air density
ω = frequency, rad/s
Φ = transition matrix representation for a digital system
Γ = input matrix representation for digital system
τ = time

State-Space Subscripts

a = actuator
c = controller
p = plant
s = sensor

Received Aug. 26, 1985; presented as Paper 85-3090 at the AIAA/AHS/ASEE Aircraft Design Systems and Operations Meeting, Colorado Springs, CO, Oct. 14–16, 1986; revision received June 27, 1986.

*Aerospace Engineer, Structures Division, Flight Dynamics Laboratory. Associate Fellow AIAA.
†Aerospace Engineer, Structures Division, Flight Dynamics Laboratory. Senior Member AIAA.
‡Aerospace Engineer, Flight Control Division, Flight Dynamics Laboratory. Member AIAA.

Introduction

STRUCTURAL dynamics, flight controls, and unsteady aerodynamics are independent technical disciplines in which significant study and research has been and is, currently, being pursued. In structures design technology, significant advances in materials and enhanced design techniques have resulted in improvements in overall aircraft structural efficiency. For flight controls, high authority automatic control systems have made modern aircraft more responsive. Unfortunately, the advances in the structural design and controls technologies were made without full consideration of each other. As a result, severe interactions between structures and controls have been encountered on some contemporary air-

craft. *The potential for aeroservoelasticity* (ASE) *exists whenever a vehicle motion sensor drives a flight control system.*

Two studies that spurred significant interest in predicting and preventing these types of instabilities involved the YF-16[1] and the YF-17[2] prototypes. Following these experiences, studies were undertaken to define procedures and criteria for avoiding ASE problems.[3-6] With the trend toward the use of high-gain, high-response flight control systems and very flexible structures, it has become clear that structural dynamics, controls, and aerodynamics must be treated in an interactive manner during the aircraft design process. If ASE instabilities are to be avoided, a common terminology and procedure need to be developed.

Structural dynamicists alone should not and probably cannot address sophisticated flight controls representations. Similarly, control systems analysts alone should not address sophisticated structural dynamics models where interactions occur. For instance, empirical corrections have been used in flight controls design to account for vehicle flexibility. It is no longer safe to assume that corrections to the static behavior of rigid body dynamics in a flight controls analysis is sufficient to account for the effects of flexibility where ASE is involved. Furthermore, a common practice has been to avoid ASE considerations until the final design analysis and a precise model is available. It is not wise to design an active flight control system without investigating ASE, even if the intent is to address modal feedback with notch filters at some later date.

The key to the successful avoidance of ASE is the assimilation of, and communication between, structural dynamics and controls with appropriate models at the appropriate design stages. Assimilation involves the creation of a common computer procedure. Communication involves the exchange of ideas and testing them with assimilated ASE procedures. The Flight Dynamics Laboratory is now working on assimilating such a computer procedure. This computer program, ADAM, is capable of analyzing aircraft with either analog or digital multi-input/multi-output (MIMO) flight control systems. The objectives of this effort are: 1) to improve the government's capability to perform analyses for auditing ongoing aircraft development programs and for evaluating proposals of advanced aircraft designs from an ASE consideration and 2) to establish a closer working relationship and to improve communication among structural dynamics, controls, and aerodynamics engineers. The next section presents the governing equations, which combine the technical disciplines into an integrated mathematical model useful for ASE evaluations.

Assimilation of Equations

ADAM is designed to integrate linear models, which were developed using well established engineering packages from each discipline, and to perform system stability analyses using either Laplace or digital domain techniques. The procedure is to transform the differential equations of motion into state-space form. The consolidated state-space representation of the integrated vehicle system is used to establish the margins of stability relative to control system parameters and flight conditions. Figure 1 presents a schematic showing the various analysis levels contained in ADAM. The dashed areas represent planned or ongoing activities to add to, or to improve, the capabilities of ADAM. A brief theoretical overview of each discipline associated with ASE follows.

Structural Dynamics

The forced aeroelastic equations of motion,

$$[M_{ss}]\{\ddot{q}_s\}+[C_{ss}]\{\dot{q}_s\}+[K_{ss}]\{q_s\}+(\rho V^2A/2)[Q_{ss}(k)]\{q_s\}=-[M_{sc}]\{\ddot{q}_c\}-(\rho V^2A/2)[Q_{sc}(k)]\{q_c\} \quad (1)$$

define the plant in ADAM. The generalized coordinates $\{q_s\}$ represent the rigid body and elastic modes that were used to define the generalized properties of the system, and $\{q_c\}$ represent the rigid control surface rotations. Generalized mass, damping, and stiffness are input to represent the structure. Typically, those modes associated with flutter instabilities and those that are within the bandwidth of the flight control system are included. These normally would include the wing bending and torsion modes, the fuselage bending modes, and the empennage modes. For the models presented in this paper, modal truncation was exercised. Modal reduction to only the low frequency modes was accomplished such that significant accuracy in the stability calculations was not lost.

To perform an ASE analysis, a consistent set of equations is required. Typically, the aeroelastic equations are formulated in the k (reduced frequency) domain and control systems are developed in either the s (continuous) or the z (discrete) domain. To merge a frequency domain flutter model with a continuous and/or discrete control model, all equations are cast in either the s-plane or the z-plane depending on whether the flight control system is analog or digital. For the immediate purposes of explanation, the s-plane equations are formulated in some detail while the z-plane approach is only summarized.

Unsteady Aerodynamics

By taking the Laplace transform of Eq. (1), assuming zero initial conditions, the aeroelastic equations of motion are transformed into functions of the complex variable, s. This results in

$$\left(s^2[M_{ss}]+s[C_{ss}]+[K_{ss}]+\frac{\rho V^2A}{2}[Q_{ss}(s)]\right)\{q_s(s)\}=\left(-s^2[M_{sc}]-\frac{\rho V^2A}{2}[Q_{sc}(s)]\right)\{q_c(s)\} \quad (2)$$

The problem of transforming a limited set of frequency dependent aerodynamics, which are in tabular form for use in Eq. (1), into the continuous complex plane or polynomial form as needed for Eq. (2) requires a curve fitting technique. Generalized unsteady aerodynamic force coefficients in the reduced frequency domain are input to ADAM and transformed into the complex domain using a least squares method and Pade polynomial approximations.[7] Equation (3) is an example of a Pade polynomial with a fourth order numerator and a second order denominator.

$$Q_{ij}(k)=\left(\frac{N_0+N_1(ik)+N_2(ik)^2+N_3(ik)^3+N_4(ik)^4}{1+D_1(ik)+D_2(ik)^2}\right)_{ij} \quad (3)$$

The coefficients N_i and D_i of the polynomials are determined by minimizing the error between the input $Q_{ij}(k)$ and its continuous approximation. Following the curve fit of each generalized force element, the denominator polynomials are averaged to define a single denominator polynomial.[8] The least squares procedure is then repeated with the denominator constrained to the average value to obtain the final numerator coefficients.

By allowing $ik=bs/V$ (imaginary axis of the s-plane), the expression for $Q_{ij}(s)$ becomes

$$Q_{ij}(s)=\left(N_0+N_1\left(\frac{bs}{V}\right)+N_2\left(\frac{bs}{V}\right)^2+N_3\left(\frac{bs}{V}\right)^3+N_4\left(\frac{bs}{V}\right)^4\right)_{ij}\Big/1+D_1\left(\frac{bs}{V}\right)+D_2\left(\frac{bs}{V}\right)^2 \quad (4)$$

Equation (4) is most accurate along the imaginary axis (valid for simple harmonic motion) and loses accuracy elsewhere in

the s-plane (damped motion). This is analogous to a k flutter solution when the damping is not zero. Aerodynamics for all rigid body and elastic modes, including control surfaces, are approximated simultaneously.

The capability to determine Pade approximations of any order such that the sum of numerator and denominator terms does not exceed 15 has been incorporated into ADAM. The program was written to allow the user to subdivide the reduced frequency range and determine Pade polynomials for each region. This feature improves the accuracy of the curve fit and minimizes the order of the aerodynamic approximation, resulting in a lower order control problem.

State-Space Representation

The aeroelastic equations of motion can be transformed into Eq. (5) by combining Eqs. (2) and (4). The equations of motion now have been transformed into a consistent set of equations in the complex plane.

$$([I]s^4 + [a_3]s^3 + [a_2]s^2 + [a_1]s + [a_0])\{q_s(s)\}$$

$$= ([b_4]s^4 + [b_3]s^3 + [b_2]s^2 + [b_1]s + [b_0])\{q_c(s)\} \quad (5)$$

Since a state-space form of the differential equations is well suited for multidisciplinary analysis, Eq. (5) is transformed back to the time domain and put in the state-space form using techniques defined in many control theory texts.[9] The unaugmented aeroelastic equations, Eq. (1), now appear as

$$\{\dot{x}_p\} = [A_p]\{x_p\} + [B_p]\{u_p\} \quad (6)$$

$$\{y_p\} = [C_p]\{x_p\} + [D_p]\{u_p\} \quad (7)$$

$$\{u_s\} = [\bar{C}]\{y_p\} \quad (8)$$

The generalized coordinates, $\{q_s\}$, and their time derivatives are represented by $\{x_p\}$, and the control surface displacements, $\{q_c\}$, and their derivatives, by $\{u_p\}$. The $[A_p]$ matrix contains the aircraft characteristics, including the structural dynamics, and unsteady aerodynamics. An eigenvalue analysis of Eq. (6) with $\{u_p\} = 0$ would provide flutter results without controls. The $[B_p]$ matrix describes the influence that the control surfaces have on the vehicle dynamics. This matrix is necessary when simulation or system integration studies are to be performed. The $[C_p]$ matrix identifies which of the system states represent the output. The $[\bar{C}]$ matrix is the modal participation coefficient matrix. This matrix defines the amount that each mode participates in the motion of the vehicle at a sensor location (modal values at each of the sensors). $[D_p]$ is a feed forward matrix. It is required whenever a transfer function has a numerator polynomial the same order as the denominator polynomial. In the case of Eq. (5), a $[D_p]$ matrix is required if $[b_4]$ is non-zero (mass coupling between the control surface and the structure, and/or unsteady aerodynamic forces).

Flight Control System

In ADAM, the MIMO flight control system is defined by segments which could be labeled sensor, controller, or actuator. Each segment is input in the form of a series of transfer function blocks. Block connectivity within each segment is input in algebraic form. After assembling the blocks to define the MIMO transfer function matrix of each segment, these equations are transformed to state-space form. These equations are similar to Eqs. (6-8), with the exception that the feed forward matrix for the actuator, $[D_a]$, is zero and $[\bar{C}]$ is an identity matrix for all control system components. Figure 2 provides a block diagram of the combined system showing the relationship between the unaugmented aircraft and the three control system segments. Combining the control segment equations with the unaugmented state equations results in the

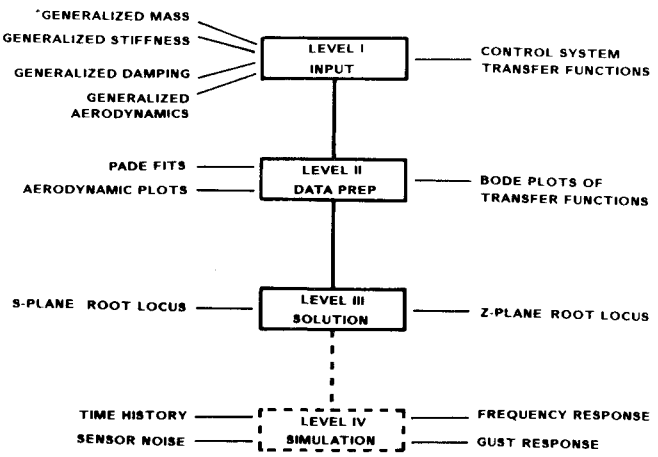

Fig. 1 Fundamental flow diagram for ADAM.

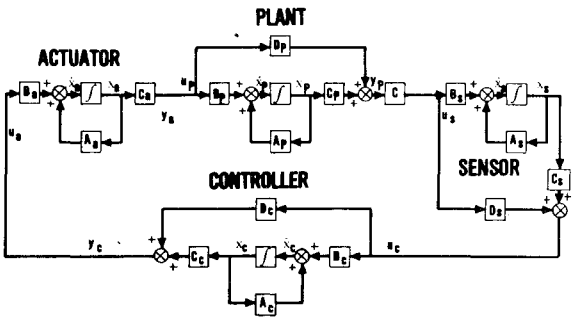

Fig. 2 Block diagram of state-space equations.

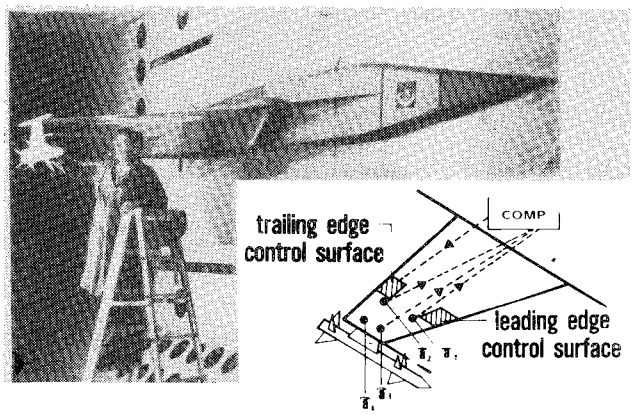

Fig. 3 Flight Dynamics Laboratory active flutter suppression wind tunnel model.

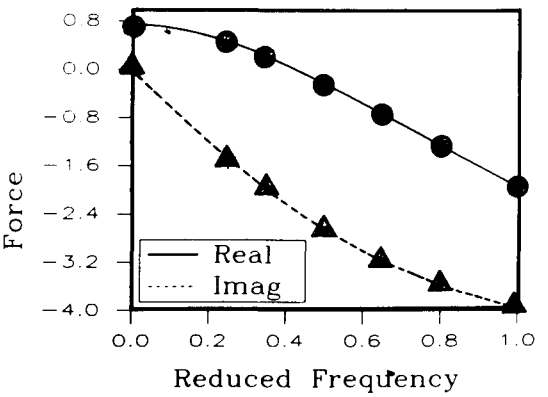

Fig. 4 Pade approximation for the control surface/wing torsion generalized force.

closed loop state representation, Eq. (9), required for evaluating the aircraft stability.

$$\begin{Bmatrix} \dot{x}_p \\ \dot{x}_s \\ \dot{x}_c \\ \dot{x}_a \end{Bmatrix} = \begin{bmatrix} A_p & 0 & 0 & B_pC_a \\ B_s\bar{C}C_p & A_s & 0 & B_s\bar{C}D_pC_a \\ B_cD_s\bar{C}C_p & B_cC_s & A_c & B_cD_s\bar{C}D_pC_a \\ B_aD_cD_s\bar{C}C_p & B_aD_cC_s & B_aC_c & A_a+B_aD_cD_s\bar{C}D_pC_a \end{bmatrix} \begin{Bmatrix} x_p \\ x_s \\ x_c \\ x_a \end{Bmatrix} \tag{9}$$

Frequency response data relating any output with any input is obtained using

$$[F(\omega)] = [F_a(\omega)][F_c(\omega)][F_s(\omega)][\bar{C}][F_p(\omega)] \tag{10}$$

where each of the segment frequency responses can be calculated in a fashion similar to that shown below,

$$[(F_p(\omega)] = [C_p][i\omega I - A_p]^{-1}[B_p] + [D_p] \tag{11}$$

From this information, Bode plots or Nyquist plots are obtained.

Digital Control Integration

For a continuous system representation in state-space form, the system response due to input u is given by

$$\{x(t)\} = [e^{[A](t-t_0)}]\{x(t_0)\} + \int_{t_0}^{t} [e^{[A](t-\tau)}][B]\{u(\tau)\}d\tau \tag{12}$$

Equation (12) can be represented as a discretized system in the time domain as

$$\{x(n+1)\} = [\Phi]\{x(n)\} + [\Gamma]\{u(n)\} \tag{13}$$

The matrix $[\Phi]$ is defined as the state transition matrix; this matrix relates the state at time $t = (n+1)T$ in terms of the state at time $t_0 = nT$ and the system input. There are many methods for determining the state transition matrix and the input matrix $[\Gamma]$. The method most suitable for ASE is the modal method due to reliability and predictable convergence. Equation (13) can be transformed into the z-domain using z transforms to obtain

$$\{x(z)\} = [z[I] - [\Phi]]^{-1}[\Gamma]\{u(z)\} \tag{14}$$

In ADAM, all segments that are continuous are transformed to the z-domain just described. Those digital segments which are already represented in the z-domain are incorporated along with the plant dynamics into an equation in the same form as Eq. (9). This equation can be solved for the z-roots and plotted in the z-domain, or the results can be transformed back to the s-plane using the identity

$$z = e^{sT} \tag{15}$$

Test Cases

In order to exercise ADAM, several examples were considered. These examples include two wind tunnel models and the unaugmented X-29A. The wind tunnel models were selected because their dynamics and control characteristics were relatively small and could be easily traced during an analysis. The X-29A was selected for its complexity and its representative status of high performance aircraft. The X-29A analysis presented in this paper addresses only the passive system and does not include the control system. The following information summarizes the results of the analyses accomplished.

FDL Flutter Suppression Model

The FDL model[10] (YF-17) has been tested in the NASA-Langley 16-ft transonic dynamics tunnel several times in the last few years to investigate analog, digital, and adaptive wing-store flutter suppression algorithms. This model was selected as an example for two reasons. First, there is a significant data base available in the literature highlighting the activities associated with the model. Second, this model required only a simple structural and control representation to predict the dynamics of the open and closed loop system. The configuration analyzed consisted of an AIM-7S missile mounted near the wing tip on an underwing pylon (Fig. 3). Only the 1st bending (4.6 Hz) and the 1st torsion (7.07 Hz) modes were needed to predict the flutter characteristics of the model accurately.

At Mach 0.8, the passive flutter characteristics of the model were calculated to be 379 ft/s at a frequency of 6.3 Hz using a doublet lattice aerodynamic representation[11] and FASTOP,[12] which are based in the frequency domain. This speed was about 1% high compared to the test results.[10] Using the Pade approximations and the state-space formulation in ADAM, the flutter speed was predicted to occur at 376 ft/s at a frequency of 6.3 Hz. The polynomial fit used for this configuration consisted of a 4th order numerator over a 2nd order denominator. A comparison of the input data for a typical force element and the resulting polynomial fit is provided in Fig. 4. The solid symbols represent the tabulated input data. All generalized forces for this configuration were approximated to the degree of accuracy shown in the figure. The velocity root locus for the passive model is provided in Fig. 5.

An optimal control law developed for the reduced order system (two modes) was studied. Actuator and sensor dynamics and several structural filters, which were neglected in the design of the optimal control law, were included in the present analyses. The sensors used by the system (referring to Fig. 3) include torsion angle and velocity, and bending angle and velocity. These signals are obtained through the integration of accelerations involving $(\bar{a}_1 - \bar{a}_2)/\ell_{12}$ for torsion and $(\bar{a}_3 - \bar{a}_1)/\ell_{31}$ for bending, respectively. The trailing-edge control surface was used as the force producer for this problem.

Figure 6 presents the velocity root locus for the augmented case. ADAM predicts instability at speeds above 781 ft/s at 3.4 Hz and at speeds below 377 ft/s at 6.7 Hz. These results agree very well with the calculations performed using frequency domain techniques which predicted corresponding speeds at 778 ft/s (3.4 Hz) and 380 ft/s (6.7 Hz), respectively. Calculations were also performed for this configuration using the digital techniques outlined earlier. These results, when converted back to the s-domain, Eq. (15), agree very well with the results shown in Figs. 5 and 6 for representative sampling times.

It is noteworthy that this active flutter suppression model is only stable in the range 380 ft/s–778 ft/s. Low-speed instabilities are not uncommon when an optimal control law is designed for a specific flight condition. An optimal control law provides excellent characteristics at speeds near the design condition but tend to become less effective at off-design conditions. This indicates the need for scheduling the gains if control is required over a large speed range. For flutter suppression, control is not important at low speeds and the control law can be deactivated. For the FDL model analyses, an instability is predicted at a speed slightly above the passive flut-

ter condition with the system operating. This instability was not a result of the system's inability to suppress flutter, but was caused by the system driving the torsion mode unstable (ASE). Without the actuator, sensor, and filter transfer functions included in the analysis, the instability boundary was much lower and the control law could be used in a conventional manner (disengaged until required). This emphasizes the importance of including all known transfer functions (actuators, sensors, filters, etc.) in the design of optimal control laws. The degrading effect of these functions could be critical at certain flight conditions.

This particular example investigated a control law that involved a single input (trailing edge control surface) with multiple outputs (three sensors). The results of this analysis agreed very well with data that was obtained from other analysis procedures. This correlation provided confidence that ADAM was performing as expected. In order to further demonstrate the accuracy and usefulness of ADAM, a slightly more complex MIMO control system was investigated.

FSW Cantilever Wing

Figure 7 shows a photograph of a forward-swept wing model mounted in the AFIT 5-ft subsonic wind tunnel. This model has been tested several times to investigate composite laminates[13] and external store effects on the aeroelasticity of forward swept surfaces. A cantilever wing configuration with mass ballast to lower the bending-torsion flutter speed into the vicinity of the wing divergence speed, was previously studied by Noll et al.[8] and was selected for the evaluation of ADAM.

The generalized properties of the passive model representation involved the three lowest flexible modes (1st bending at 2.4 Hz, 2nd bending at 12.6 Hz, and 1st torsion at 23.6 Hz). The aerodynamics for these modes and for two control surface rotation modes were calculated using the doublet lattice method. Flutter analyses predicted instabilities at 119 ft/s (divergence) and at 155 ft/s at 16.9 Hz (flutter). Results from ADAM found the divergence speed at 117 ft/s and the flutter speed at 154 ft/s (17.0 Hz). The agreement between the two methods is very good, indicating that the aeroelastic equations within ADAM are formulated correctly and that the aerodynamic fits were satisfactory. A velocity root locus for this model with the control system off is presented in Fig. 8.

A schematic of the wing and control system for this example is presented in Fig. 9. This system has two independent feedback loops. The divergence suppression system consists of the leading-edge control surface commanded by wing bending displacement times a negative gain. Wing tip angular acceleration is used as a feedback variable for suppression of flutter by the trailing-edge control surface. The compensation for this system consists of a gain and a phase lag network. Figure 10 shows the velocity root locus plot with both loops closed. ADAM predicts an instability in the 2nd elastic mode at 191 ft/s at 12.4 Hz. Previous calculations[8] predicted an instability at 188 ft/s at a frequency of 12.7 Hz. These comparisons provide confidence that a MIMO system is formulated correctly in ADAM.

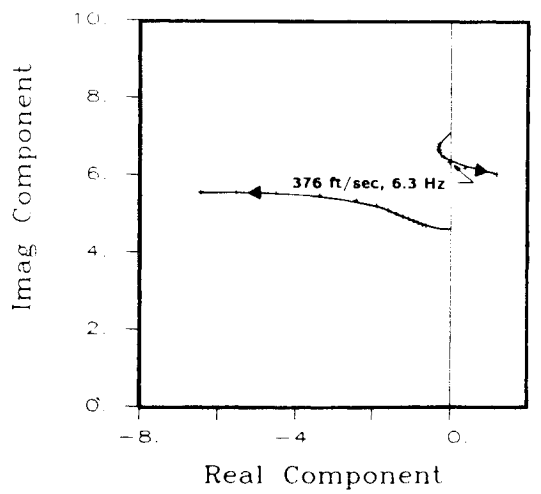

Fig. 5 Velocity root locus for the Flight Dynamics Laboratory flutter suppression model, passive case.

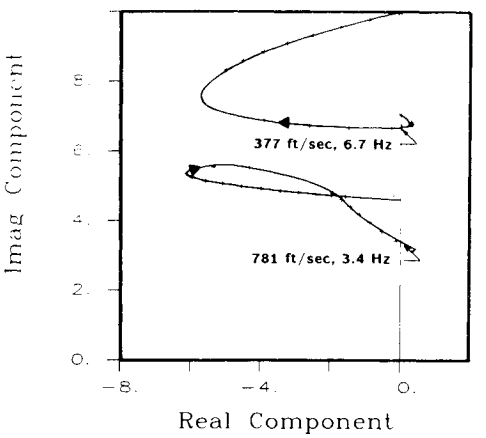

Fig. 6 Velocity root locus for the Flight Dynamics Laboratory flutter suppression model, augmented case.

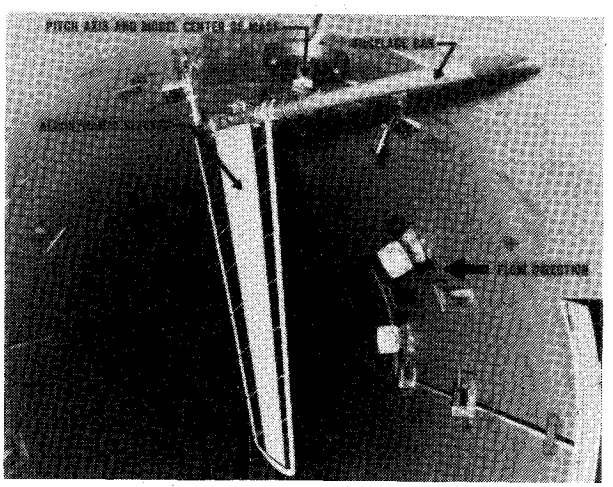

Fig. 7 Cantilever forward-swept wing wind tunnel model.

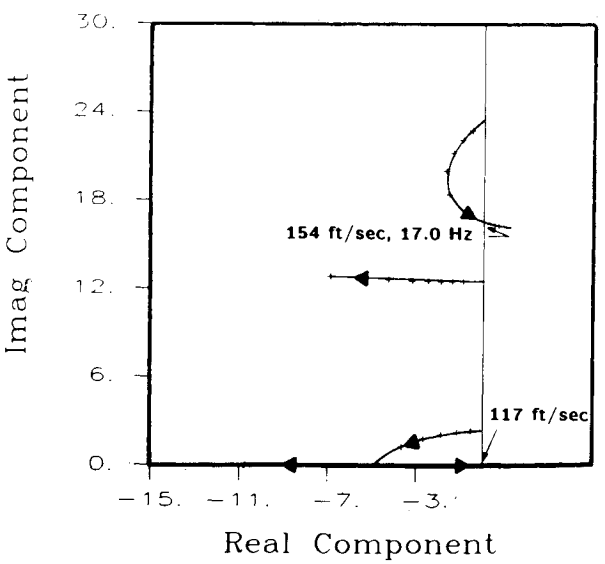

Fig. 8 Velocity root locus for the cantilever forward-swept wing model, passive case.

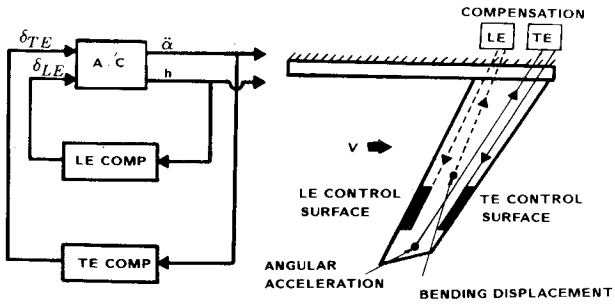

Fig. 9 Schematic of control system for the cantilever forward-swept wing model.

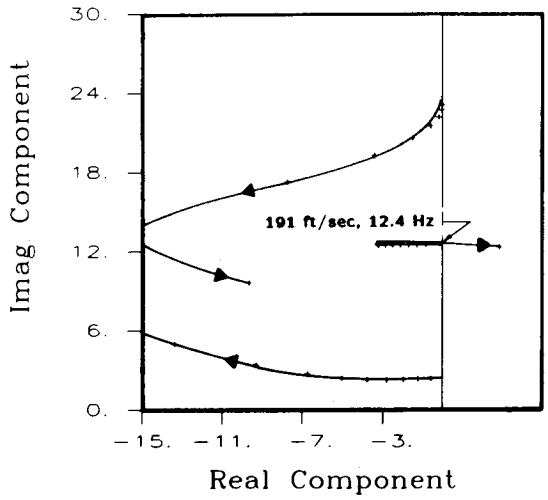

Fig. 10 Velocity root locus for the cantilever forward-swept wing model, augmented case.

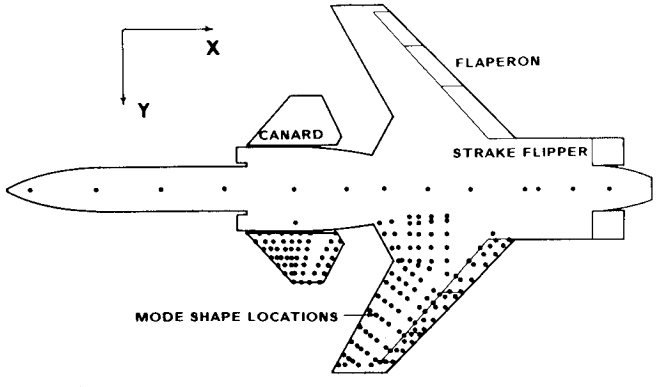

Fig. 11 X-29A structural dynamics model discretization.

X-29A Aircraft

The X-29A aircraft provides a relatively complex design with a digital control system to stabilize a relaxed static stability configuration. This aircraft exhibits the type of ASE challenges most likely to be found for future designs. Sensors located in the vehicle fuselage for the purpose of feeding back longitudinal pitch and plunge also feed back structural deformations, creating the possibility of ASE instabilities. The active surfaces include the wing trailing-edge control surfaces, the canards, and the strake flaps.

Figures 11 and 12 present the structural and aerodynamic representations, respectively, of the X-29A used for the longitudinal mode. The FASTOP computer program was used to obtain the doublet lattice aerodynamics at a Mach number of 0.9 for two rigid body, 15 elastic, and three control surface rotation modes. Although this information is adequate for

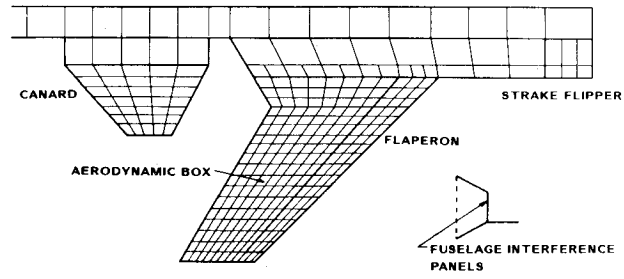

Fig. 12 X-29A aerodynamic model discretization.

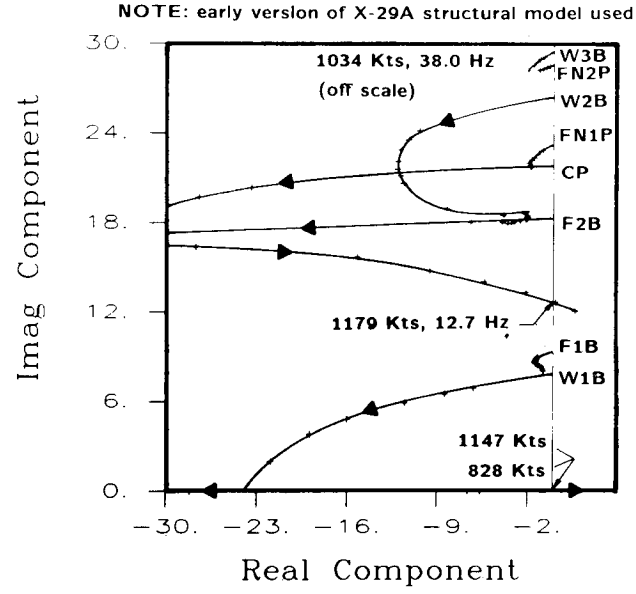

Fig. 13 Velocity root locus for the X-29A, passive case (15 symmetric modes, $M=0.9$).

evaluating ADAM, the results are not to be used to draw conclusions concerning the actual aircraft. The X-29A math model used for these calculations does not reflect any of the design revisions that have taken place in the last several years nor has it been updated based on the ground vibration tests.

A FASTOP analysis[14] with free-free flexible modes without the rigid body modes explicity included predicted wing divergence at 817 knots and canard divergence at 1151 knots. Flutter instabilities were found at 1011 knots (38.1 Hz) for the canard and at 1186 knots (12.6 Hz) for the wing. Figure 13 provides a velocity root locus plot obtained from ADAM without the active systems included in the analyses for the elastic modes up through 30 Hz. Comparison between the instability speeds and frequencies presented on the figure with the FASTOP data shows excellent agreement.

Future Work

At the present time, ADAM is configured to perform root locus analyses on a series of preselected scheduled flight conditions and control system gains. It is expected that, as adaptive flight controls are incorporated into flexible aircraft, the process of certification relative to ASE will involve unlimited combinations of control gains and flight conditions that must be analyzed. This problem and others will be explored, and new approaches to the area of ASE analysis will be defined.

Transformation of the rigid body motion from Newtonian coordinates (space-fixed) to body-fixed coordinates would facilitate flexible vehicle flight simulation. It is expected that vehicle rigid body dynamics will not appreciably affect the choice of generalized modal coordinates to represent flexible vehicle behavior. There are plans to investigate this transformation in ADAM in the near future.

In addition to the above topics, other improvements to ADAM, which will be investigated, include the following: 1) Pilot inputs for aircraft stability and control evaluations; 2) gust inputs for aircraft response studies; 3) sensor noise or other component disturbances for robustness considerations; 4) real time simulation capability using nonharmonic subsonic unsteady aerodynamics; 5) analysis with transonic aerodynamics.

Conclusions

Merging aerodynamics, controls, and structural dynamics into a single unified ASE analysis requires a tedious process of organization and assimilation that would be all but impossible without the aid of a computer program. Since the aircraft design process and mathematical modeling is unique to each aircraft manufacturer, it is expected that the merging of disciplines into an ASE analysis will also be unique to each aircraft manufacturer. Thus, the basics of ASE analyses are given in this paper in order to encourage readers to develop and incorporate this multidiscipline analysis into their own design process. *ASE must be considered in any aircraft design where flexibility and high speed are combined with high-gain active control systems.* As a result, ASE is anticipated to become a critical design factor for the next generation of USAF fighter aircraft.

Program ADAM was the result of an initial investigation to address the multidiscipline area of aeroservoelasticity. The software was prepared using the VAX 11/785 computer with a VMS operating system. The theoretical manual and the user's guide for ADAM are provided in Ref. 15.

References

[1]Peloubet, R. P., "YF-16 Active Control System/Structural Dynamics Interaction Instability," AIAA Paper 75-823, May 1975.

[2]Arthurs, T. D. and Gallagher, J. T., "Interaction Between Control Augmentation System and Airframe Dynamics on the YF-17," AIAA Paper 75-824, May 1975.

[3]Barfield, A. F. and Felt, L. R., "Aeroservoelasticity—A Merging of Technologies," Society of Flight Test Engineers 7th Annual Symposium, Eastsound, WA, Aug. 1976.

[4]Peloubet, R. P., Haller, R. L., Cunningham, A. M., Cwach, E. E., and Watts, D., "Application of Three Aeroservoelastic Stability Analysis Techniques," AFFDL-TR-76-89, Sept. 1976.

[5]Felt, L. R., Huttsell, L. J., Noll, T. E., and Cooley, D. E., "Aeroservoelastic Encounters," *Journal of Aircraft*, Vol. 16, July 1979, pp. 477-483.

[6]"Proceedings of the Aeroservoelastic Specialists Meeting," AFWAL-TR-84-3105, Oct. 1984.

[7]Vepa, R., "On the Use of Pade' Approximants to Represent Unsteady Aerodynamic Loads for Arbitrary Small Motions of Wings," AIAA Paper No. 76-17, Jan. 1976.

[8]Noll, T. E., Eastep, F. E., and Calico, R. A., "Active Suppression of Aeroelastic Instabilties for Forward Swept Wings," AFWAL-TR-84-3002, Dec. 1983.

[9]D'Azzo, J. J. and Houpis, C. H., *Linear Control System Analysis and Design: Conventional and Modern*, McGraw-Hill, New York, NY, 1st Ed. 1975.

[10]Hwang, C., Winther, B. A., Mills, G. R., Noll, T. E., and Farmer, M. G., "Demonstration of Aircraft Wing/Store Flutter Suppression Systems," *Journal of Aircraft*, Vol. 16, Aug. 1979, pp. 557-563.

[11]Giesing, J. P., Kalman, T. P., and Rodden, W. P., "Subsonic Unsteady Aerodynamics for General Configurations," AFFDL-TR-71-5, Nov. 1971.

[12]Markowitz, J. and Isakson, G., "FASTOP-3: A Strength, Deflection and Flutter Optimization Program for Metallic and Composite Structures," AFFDL-TR-78-50, May 1978.

[13]Sherrer, V. C., Hertz, T. J., and Shirk, M. H., "Wind Tunnel Demonstration of Aeroelastic Tailoring Applied to Forward Swept Wings," *Journal of Aircraft*, Vol. 18, Nov. 1981, pp. 976-983.

[14]Blair, M. and Noll, T. E., "X-29A Aeroelastic Analysis Model, Vibration and Flutter Analysis," AFWAL-TM-85-198-FIBR, March 1985.

[15]Blair, M. and Noll, T. E., "A Procedure for Aeroservoelastic Analyses Involving Aircraft with Analog or Digtial Control Systems," Vol. I: "Theoretical Manual" and Vol. II: "User's Manual," AFWAL-TR-86-3040, (to be published).